Peer-reviewed version available at *Pharmaceutics* **2019**, *11*, 86; doi:10.3390/pharmaceutics11020086

Article

Chitosan-Coated Nanoparticles: Effect of Chitosan Molecular Weight on Nasal Transmucosal Delivery

Franciele Aline Bruinsmann [1,2], Stefania Pigana [2], Tanira Aguirre [3], Gabriele Dadalt Souto [1], Gabriela Garrastazu Pereira [1], Annalisa Bianchera [2], Laura Tiozzo Fasiolo [2,4], Gaia Colombo [4], Magno Marques [5], Adriana Raffin Pohlmann [1,6], Silvia Stanisçuaski Guterres [1] and Fabio Sonvico [2,*]

[1] Programa de Pós-Graduação em Ciências Farmacêuticas, Universidade Federal do Rio Grande do Sul, Porto Alegre 90610-000, Brazil; fbruinsmann@gmail.com (F.A.B.); gabrieledadalt@gmail.com (G.D.S.); garrastazugp@gmail.com (G.G.P.); silvia.guterres@ufrgs.br (S.S.G.); adriana.pohlmann@ufrgs.br (A.R.P.);
[2] Food and Drug Department, University of Parma, Parco Area delle Scienze 27/a, 43124 Parma, Italy; stefania.pigana@studenti.unipr.it (S.P.); annalisa.bianchera@unipr.it (A.B.)
[3] Programa de Pós-Graduação em Biociências, Universidade Federal de Ciências da Saúde de Porto Alegre, Porto Alegre, RS 900500-170, Brazil; tanira@ufcspa.edu.br
[4] Department of Life Sciences and Biotechnology, University of Ferrara, Via Fossato di Mortara 17/19, 44121 Ferrara, Italy; laura.tiozzofasiolo@studenti.unipr.it (L.T.F.); clmgai@unife.it (G.C.)
[5] Instituto de Ciências Biológicas, Universidade Federal do Rio Grande, Rio Grande, RS 96203-900, Brazil; magnomarques@aol.com
[6] Departamento de Química Orgânica, Instituto de Química, Universidade Federal do Rio Grande do Sul, Porto Alegre 91501-970, Brazil

* Correspondence: fabio.sonvico@unipr.it; Tel.: +39-0521-906-282

Abstract: Drug delivery to the brain represents a challenge especially in the therapy of central nervous system malignancies. Simvastatin (SVT), as other statins, has shown potential anticancer properties that are difficult to exploit in the CNS. In the present work the physico-chemical, mucoadhesive and permeability enhancing properties of simvastatin-loaded poly-ε-caprolactone nanocapsules coated with chitosan for nose-to-brain administration were investigated. Lipid-core nanocapsules coated with different molecular weight (MW) chitosans (LNC_{chit}) prepared by a novel one-pot technique were characterized for particle size, surface charge, particle number density, morphology, drug encapsulation efficiency, interaction between surface nanocapsules with mucin, drug release and permeability across two nasal mucosa models. Results show that all formulations present adequate particle size (below 220 nm), positive surface charge, narrow droplet size distribution (PDI<0.2) and high encapsulation efficiency. Nanocapsules presented controlled drug release and mucoadhesive properties dependent on the MW of the coating chitosan. The results of permeation across RPMI 2650 human nasal cell line evidenced that LNC_{chit} increased the permeation of SVT. In particular, the amount of SVT permeated after 4h for nanocapsules coated with low MW chitosan, high MW chitosan and control SVT was 13.91 ± 0.78 μg, 9.15 ± 1.23 μg and 1.42 ± 0.21 μg respectively. These results were confirmed by the SVT *ex vivo* permeation across rabbit nasal mucosa. This study highlighted the suitability of LNC_{chit} as promising strategy for the administration of simvastatin for a nose-to-brain approach for the therapy of brain tumors.

Keywords: nasal permeability; nose-to-brain; simvastatin; nanocapsules; mucoadhesion; CNS disorders; chitosan

1. Introduction

Statins are potent inhibitors of the hydroxymethyl glutaryl coenzyme A (HMG-CoA) reductase, commonly administered for the treatment of cardiovascular disease [1]. However, in recent years, it

has been suggested that the statin therapeutic indications might expand due to their pleiotropic effects [2]. These non-cholesterol related effects include their modulation of immune responses, the enhancement of endothelial function, the reduction oxidative stress and the check of inflammation processes [3,4]. The majority of pleiotropic effects are mediated by preventing the synthesis of isoprenoids and subsequent inhibition of small signaling proteins [5,6]. Among the diseases that could benefit from statins pleiotropic effects are multiple sclerosis, rheumatoid arthritis, systemic lupus erythematosus, chronic obstructive pulmonary disease, neurodegenerative disorders, bacterial infections and cancer [3].

In the field of cancer therapy, statins showed pro-apoptotic effects against various tumor cell lines [7,8] and numerous studies have examined their potential chemopreventive action [9]. Due to the inhibition of the enzyme HMG-CoA reductase, statins decrease the levels of mevalonate, the precursor of dolichol, geranylpyrophosphate (GPP) and farnesyl-pyrophosphate (FPP). Dolichol enhances DNA synthesis and is associated to several proteins found in tumor cells [10]. GPP and FPP are post-translational modifications of intracellular proteins as G-proteins Ras and Rho that regulate the signal transduction of several membrane receptors and are critical for the transcription of genes involved in cell proliferation, differentiation, and apoptosis. Ras and Rho gene mutations are found in a variety of tumor cells [11,7]. Furthermore, statins show apoptotic effect in human glioblastoma cell lines inducing depletion of geranylgeranylated proteins, important for the transition to the cell cycle phases [12]. Statins have also shown to play a role in the prevention of tumor metastases by inhibition of epithelial growth factor–induced tumor cell invasion [13]. Moreover, statins, inducing the inactivation of nuclear factor kB, reduce urokinase and matrix metalloproteinase-9 expression, pivotal for tumor metastatic process [7,14]

In the case of glioma cell lines, simvastatin (SVT) showed suppression of cell proliferation and induction of apoptosis [15,16]. However, when evaluated in an *in vivo* orthotopic model of glioblastoma multiforme model, simvastatin did not show tumor inhibitory effects [17]. As in this experiment, the major factor for failure of chemotherapies against central nervous system (CNS) tumors has been attributed to limited brain-blood barrier (BBB) permeability [18]. In addition, after oral administration statins are extensively metabolized in the liver and their hydrophilic metabolites are prevented from crossing the BBB [19].

Some new strategies have been proposed to deal with such limitations in order to increase distribution of drugs in the CNS, like the use of nose-to-brain route [20,21] and the development of nanocarriers [22, 23, 24]. In recent years, the nose-to-brain delivery has attracted much attention as a mean to deliver drugs more efficiently to the CNS bypassing the BBB. This is because the nasal cavity is anatomically connected to the CNS via the olfactory system [25]. Moreover, it offers advantages such, non-invasiveness, avoidance of hepatic first-pass metabolism, practicality and convenience of administration [26]. However, due to the presence of rapid mucociliary clearance mechanism, nasal delivery application for brain delivery is hindered by the short residence time of conventional formulations. Moreover, the barrier of the nasal epithelium, nasal metabolism and the limited volume of administration are limiting aspects for the development of nose-to-brain drug delivery systems [25,27].

To increase bioavailability after nasal delivery, polymeric nanocapsules have been investigated [28, 29, 30]. These nanocarriers are considered a type of reservoir drug delivery system [31] and can be obtained by interfacial deposition of pre-formed polymers [32]. Their structure is characterized by an oil core surrounded by a polymeric shell stabilized by a surfactant system [31,33]. The lipid-core nanocapsules (LNCs), developed by our research group, are composed by a dispersion of sorbitan monostearate (solid lipid) and medium chain triacylglycerol (liquid lipid) in the core, surrounded by poly(ε-caprolactone), an aliphatic polyester as polymeric wall and polysorbate 80 as stabilizing surfactant [34]. The lipid core dispersion, i.e. sorbitan monostearate dispersed in oil, confers different properties to this system as controlled the drug release and increased the encapsulation efficiency when compared to the core of the conventional nanocapsules containing only liquid lipids [34, 35, 36]. These nanocarriers showed efficient brain delivery of drugs to the brain as resveratrol [37] and curcumin [38] when administered orally and intraperitoneally, as well as reduction of side effects of

Peer-reviewed version available at Pharmaceutics 2019, 11, 86; doi:10.3390/pharmaceutics11020086

the antipsychotic drug olanzapine [39]. Furthermore, they demonstrated improved *in vitro* and *in vivo* antitumor effectiveness of resveratrol, methotrexate and acetyleugenol when compared to the free drugs [40, 41, 42].

Bender and co-authors [43], developed a two-step process to obtain modified LNC stabilized simultaneously with polysorbate 80 and lecithin and coated with chitosan. Chitosan is a cationic biopolymer obtained by the partial deacetylation of chitin under alkaline conditions [44]. Chitosan demonstrated several interesting properties for pharmaceutical application, such as biodegradability, biocompatibility, antibacterial activity and controlled release of drugs [45, 46]. Furthermore, chitosan showed mucoadhesive and penetration enhancing properties, particularly desirable for its application in drug nasal delivery [47, 48]. These actions are mediated by structural reorganization of the tight junctions of the nasal epithelium, increasing paracellular transport of drugs [49].

In the present study, LNC stabilized with lecithin and coated with chitosan were obtained by an innovated one-pot technique. Moreover, the pharmaceutical properties of formulations with chitosan of different molecular weight (MW) intended for nose-to-brain delivery of simvastatin were evaluated.

2. Materials and Methods

2.1 Materials

Poly (ε-caprolactone) (PCL) (MW=14,000) and Span 60® (sorbitan monostearate) were purchased from Sigma-Aldrich (Strasbourg, France). Caprylic/capric triglyceride was obtained from Delaware (Porto Alegre, Brazil) and simvastatin (SVT) was purchased from Pharma Nostra (Rio de Janeiro, Brazil). Chitosan low MW (21 KDa - viscosity 9 cP) and high MW (152 KDa - viscosity 114 cP) was provided by Primex (Chitoclear FG, deacetylation degree 95%, Siglufjordur, Iceland). Soybean lecithin (Lipoid S75) was kindly donated by Lipoid AG (Ludwigshafen, Germany). Minimum essential medium (MEM), fetal bovine serum (FBS), phosphate-buffered saline (PBS) and Hank's Balanced Salt Solution (HBSS) were supplied by Gibco (Carlsbad, CA, USA). Transwell® cell culture inserts (1.12 cm^2 surface area, polyester, 0.4 μm pore size) were supplied by Corning Costar (Lowell, MA, USA). All other chemicals and solvents used were of analytical or pharmaceutical grade.

2.2 Preparation of the Lipid-core Nanocapsules Coated using a One-pot Technique

Chitosan-coated simvastatin-loaded lipid-core nanocapsules were prepared according to the interfacial deposition of pre-formed polymer method already reported in literature [35]. An organic phase (25 mL of acetone) containing the polymer (PCL, 0.04 g), sorbitan monostearate (0.016 g) and caprylic/capric triglyceride (0.048 mL) was kept under magnetic stirring at 40°C. After complete dissolution of the components, an ethanolic solution (4 mL) containing lecithin (0.025 g) was added into organic phase and finally, simvastatin (0.010 g) was added and completely dissolved. The aqueous phase (50 mL) contained of 0.1% w/v of chitosan, prepared as a dilution from a 0.5% w/v of chitosan solution in 1% (v/v) acetic acid. The organic phase was injected using a funnel into the aqueous phase under moderate magnetic stirring. The solvents were eliminated at 40°C until the final volume of 10 mL, was obtained by the use of a rotary evaporator Büchi® R-114 (Flawill, Switzerland). The formulations obtained were named $LNC_{SVT\text{-}LMWchit}$ when chitosan low MW (viscosity 9 cP) was used and $LNC_{SVT\text{-}HMWchit}$ when chitosan high MW (viscosity 114cP) was used in alternative. Blank nanocapsules ($LNC_{LMWchit}$ and $LNC_{HMWchit}$) were also prepared, omitting the simvastatin from the organic phase preparation.

2.3 Drug Content and Encapsulation Efficiency

The SVT quantification was carried out by high performance liquid chromatography with detection in the ultraviolet (HPLC-UV), using a previously validated method [30]. The analysis was

Peer-reviewed version available at Pharmaceutics 2019, 11, 86; doi:10.3390/pharmaceutics11020086

performed with a Shimadzu HPLC system (Kyoto, Japan) with detection at 238 nm and using a column Phenomenex Lichrosphere® C18 (4.6.x250 mm, 5 μm). The composition of the mobile phase was 65% of acetonitrile and 35% sodium dihydrogen phosphate buffer (25 mM, pH 4.5), flow rate was 1.0 mL·min^{-1} and injection volume of 100 μL. Calibration curves (n = 3) were prepared to determine linearity (R > 0.99) in the concentration range from 0.1 to 20 μg·mL^{-1}. The drug content in the formulations was determined by diluting a precise volume of nanoparticles suspension (100 μL) in 10 mL of the mobile phase. The samples were then sonicated for 30 minutes and filtered through a 0.45 μm pore size membrane (Millipore®, Billerica, USA) before being assayed by HPLC-UV. Free simvastatin was determined in the ultrafiltrate after ultrafiltration–centrifugation (Ultrafree-MC, cut-off of 30 kDa, Millipore) at 2688×g (Scilogex D3024, Rocky Hill, CT, USA) for 15 minutes and quantified by HPLC-UV. Encapsulation efficiency (EE) as percentage was calculated by the difference between the total and free, *i.e.* non-encapsulated, drug amount divided by the total drug amount multiplied by 100. All analyses were performed for triplicate batches (n = 3).

2.4 Physicochemical Characterization

The nanoparticle formulations were characterized with multiple techniques as described below. All analyses, with the exception of the TEM (n = 1), were performed for triplicate batches (n = 3).

2.4.1 Laser Diffraction

The particle size and the size distribution were determined by laser diffraction (Mastersizer® 2000, Malvern Instruments, UK) aiming to spot the eventual presence of micrometric particles or aggregates. The sample was directly added to water in the wet dispersion accessory (Hydro 2000SM - AWM2002, Malvern Instruments, UK) until an obscuration level of 2% was reached. The particle size was then expressed using the volume-weighted mean diameter (D[4,3]), and the diameters calculated at 10, 50 and 90 percentiles [$d_{0.1}$, $d_{0.5}$ and $d_{0.9}$, respectively] of the cumulative size distribution curve by volume (v) and by number (n) of particles. The width of the distribution (Span) was determined according to Eq. 1.

$$Span = \frac{d_{0.9} - d_{0.1}}{d_{0.5}}, \quad (1)$$

2.4.2 Dynamic Light Scattering

The mean particle size (Z-average diameter) and polydispersity index (PDI) of nanocapsules were evaluated by dynamic light scattering (DLS) at 25 °C using a Zetasizer® Nano ZS (Malvern Instruments, UK). After dilution of samples (500×) in purified and filtered (0.45 μm) water, the correlogram was obtained by allowing the instrument software to determine the optimal time of acquisition and the z-average diameter and PDI were calculated by the method of Cumulants with the same software.

2.4.3 *Nanoparticle Tracking Analysis*

The nanoparticles tracking analysis (NTA) method was used to determine the mean diameter and the concentration of nanocapsules per volume, expressed as particle number density (PND) (NanoSight LM10, Malvern Pananalytical, UK). The analysis was carried out diluting the samples in ultrapure water (1000×) and introducing it into the instrument sample chamber cell by a syringe. The chamber is located on an optical microscope that using a laser diode (635 nm) illuminate the particles in suspension. The NTA 3.2 software tracks single particles, which are in Brownian motion, and can relate this particle movement with a sphere equivalent hydrodynamic radius as calculated using the Stokes–Einstein equation (Eq. 2). The samples were evaluated at room temperature for 60 seconds

Peer-reviewed version available at Pharmaceutics 2019, 11, 86; doi:10.3390/pharmaceutics11020086

with automatic detection. The results correspond to the arithmetic average of the calculated sizes of all particles analyzed.

$$\overline{(x,y)^2} = \frac{4\,Tk_B}{3\pi\eta d_h}, \quad (2)$$

Where k_B is the Boltzmann constant and $\overline{(x,y)^2}$ is the mean-squared displacement of a particle during time t at temperature T, in a medium of viscosity η, with a hydrodynamic diameter of d_h.

2.4.4 pH and Zeta Potential

The pH values of nanocapsules suspensions were determined using a calibrated potentiometer (DM-22 Digimed, São Paulo, Brazil) via direct measurements of the formulations at 25ºC. The zeta potential values were determined by electrophoretic mobility after the samples were diluted in 10 mM NaCl aqueous solution (500×) previously filtered (0.45 μm, Millipore®, Billerica, USA). The zeta potential of nanoparticles suspensions was also measured at different pH values using the MPT-2 autotitrator for the Zetasizer® Nano ZS (Malvern Instruments, Malvern, UK). The samples (10 mL) were placed in the titration cell and titrated over acidic (0.1 M HCl) towards basic (0.05 M NaOH) pH range at 1.0 pH unit intervals. This combination allowed automated titration over a wide pH range and thus made it possible to determine the isoelectric point (IEP) of nanoparticles.

2.4.5 Morphology

Transmission electron microscopy (TEM) was used to evaluate the morphology of the formulations. TEM samples were diluted in ultrapure water (10×, v/v) and then deposited (10 μL) on specimen grids (Formvar-Carbon support film, Electron Microscopy Sciences, Hatfield, PA, USA) and negatively stained with uranyl acetate solution (2% w/v, Sigma-Aldrich, St.Louis, MO, USA). Analyses were performed using a transmission electron microscope (JEM 2200-FS, Jeol, Tokyo, Japan) operating at 80 kV. The images were processed with Digital Micrograph (Gatan Inc., Pleasanton, CA, USA) software.

2.5 In Vitro Evaluation of the Interaction between Nanocapsules and Mucin

The mucoadhesive properties of the formulations were assessed using mucin from porcine stomach (Type II, Sigma-Aldrich, St. Louis, MO, USA) as previously described [29,50]. The mucin was dispersed in ultrapure water (0.5% w/v) and employing magnetic stirring for 3 h at room temperature. The suspension was centrifuged at 4000×g for 30 min. The supernatant was collected and lyophilized. Then mucin solutions were prepared in simulated nasal electrolytic solution (SNES) [51] at predetermined weight ratios f, determined as:

$$f = \frac{W_{mucin}}{W_{mucin} + WNC}, \quad (3)$$

where W_{mucin} is the mucin mass and WNC is the LNC_{chit} nanocapsules mass.

The Z-average diameter and PDI before and after contact with mucin were measured by DLS as described above after dilution (500×) of the samples in mucin solutions. The mucoadhesive index values (MI) were determined as:

$$MI = \frac{d}{d_0}, \quad (4)$$

Peer-reviewed version available at Pharmaceutics 2019, 11, 86; doi:10.3390/pharmaceutics11020086

where d and d_0 are the diameter of the LNC_{chit} nanocapsules before and after interaction with mucin, respectively.

Furthermore, changes in the zeta potential were measured after the nanocapsules were diluted (500×) in mucin solutions containing 10 mM NaCl.

2.6 In Vitro Release Study

The *in vitro* release profiles of SVT from formulations were determined using the dialysis bag method. Briefly, 1 mL of each sample was placed in a dialysis bag (14 kDa molecular weight cut-off, Sigma-Aldrich, St. Louis, MO, USA) and suspended into 100 mL of SNES containing 0.5% of polysorbate 80 to improve SVT solubility and to reach the sink conditions. A free drug solution was placed in the dialysis bag in control experiments ($SVT_{solution}$, simvastatin dissolved in 1% ethanol and 0.5% polysorbate 80). The dialysis bags were maintained in the medium under stirring and thermostated in a water bath (37 °C). One milliliter of release medium was collected at predetermined time intervals (from 0.16 to 8h) and filtered (0.45 µm, Millipore®, Billerica, USA). The volume was replaced by adding one milliliter of fresh release medium pre-heated at 37 °C. The samples were analyzed by HPLC-UV, and the cumulative drug release was determined.

2.7 Transport Studies across an in vitro Nasal Epithelial Cell Model

RPMI 2650 human nasal cells (human nasal septum tumor, ECACC, Salisbury, UK) were cultured in MEM media supplemented with 10% (v/v) fetal bovine serum (FBS). Cells were grown at 37°C in an atmosphere of 95% air/5% CO_2. Transwell® cell culture inserts were used to establish an air-liquid interface (ALI) nasal model, as previously reported [52]. Briefly, 200 uL of the cells suspensions ($2.5 \cdot 10^6$ cell/mL) were seeded on Transwell® and after 24 hours, the media from apical compartment was removed resulting in ALI culture configuration. After 14 days from seeding the Transwell® were removed and transferred to a 12-well plate containing 1.5 mL of pre-warmed HBSS. Then, 200 µL of $LNC_{SVT\text{-}LMWchit}$, $LNC_{SVT\text{-}HMWchit}$ and $SVT_{control}$ were added to the upper compartment and samples of 200 µL were collected from the baso-lateral chamber at pre-determined time points (1, 2, 3 and 4 h) and replaced with the same volume of fresh HBSS buffer. The samples were quantified for simvastatin content using HPLC-UV (n = 4). TEER measurements were performed with a Millicell-ers® (Millipore) at the beginning and at the end of experiment in order to confirm that the integrity of the cell layer was maintained.

2.8 Ex Vivo Transport Experiments across Rabbit Nasal Mucosa

The transport of simvastatin across rabbit nasal tissue was evaluated using Franz type vertical diffusion cells with a receptor volume of 4.5 mL and diffusional area of 0.58 cm^2. On the day of the experiment, nasal mucosae were freshly excised from rabbits obtained from a local slaughterhouse (Pola, Finale Emilia, Italy) and cleaned to remove adhering submucosal tissue [53]. The rabbit nasal mucosa was placed between the donor and the receptor compartment of the diffusion cells. Then, in order to check the mucosa integrity, the donor compartment was filled with medium to confirm that no liquid leaked into the cell receptor compartment. If the nasal mucosa passed this test, the donor compartment received 200 µL one among the three tested preparations, i.e. $LNC_{SVT\text{-}LMWchit}$, $LNC_{SVT\text{-}HMWchit}$ and $SVT_{control}$, equivalent to 200 µg of SVT. Franz cells were maintained at 37 °C under mild magnetic stirring. At predetermined time intervals, 500 µL of the receptor medium, SNES containing 0.5% w/v of polysorbate 80, was withdrawn and the receptor compartment refilled with an equivalent volume of fresh medium. All samples were analyzed by HPLC-UV. In order to evaluate the retention of SVT in the nasal tissue, mucosa samples were placed in a volumetric flask (10 mL) containing a solvent of extraction (acetonitrile) and subjected to vortexing (2 min) and sonication (15 min). The solvent of extraction was then filtered (0.45 µm, Millipore®, Billerica, USA) and simvastatin quantified using HPLC-UV. The experiments were conducted in triplicate for each formulation.

Peer-reviewed version available at Pharmaceutics 2019, 11, 86; doi:10.3390/pharmaceutics11020086

2.9 Preliminary Nasal Toxicity Studies

Nasal toxicity studies were performed using rabbit nasal mucosa in a similar way to *ex vivo* permeation study mentioned above in order to evaluate any damage to the mucosa. Each mucosa piece, of uniform thickness, was treated with $LNC_{SVT\text{-}LMWchit}$, $LNC_{SVT\text{-}HMWchit}$, $SVT_{control}$ and PBS pH 6.4 (negative control) by placing 200 µL in the donor compartment of Franz diffusion cells. The acceptor contained 4.5 mL of SNES containing 0.5% w/v of polysorbate 80. After 4 h, for each condition nasal mucosa was washed with PBS, fixed in 10% v/v buffered formalin for 6 h and embedded in histological paraffin. A rotatory microtome was used to perform transverse cuts to obtain sections (5 µm) that were stained with hematoxylin-eosin. Images of mucosa samples were observed using an Olympus BX51 optical microscope with attached camera DP72 (Olympus, Tokyo, Japan) [54].

2.10 Statistical Analysis

Data are presented as mean ± standard deviation (SD) of analysis of at least triplicate batches (n = 3). Statistical analysis was performed using the Student's t-test for two groups or one-way analysis of variance (ANOVA) followed by Tukey's test for multiple groups using GraphPad Prism Software 5.0 (GraphPad Software, Inc., San Diego, CA). Differences were considered significant at $p<0.05$.

3. Results

SVT-nanocapsules were prepared using the interfacial deposition of pre-formed polymer method and coated with chitosan with a one-pot technique. The surface of the NPs was coated with two different chitosan grades, characterized by different molecular weight and hence different viscosities, in order to evaluate the effect of chitosan molecular weight on the mucoadhesive properties and permeability enhancement of the nanocapsules obtained.

3.1. Characterization of nanocapsules

SVT nanocapsules appeared macroscopically like an opalescent white homogeneous dispersion. The total SVT content in the formulations was found to be 0.94 ± 0.04 $mg{\cdot}mL^{-1}$ for $LNC_{SVT\text{-}LMWchit}$ and 0.96 ± 0.02 $mg{\cdot}mL^{-1}$ for $LNC_{SVT\text{-}HMWchit}$. Regarding encapsulation efficiency (EE), SVT was not detected in the ultrafiltrate for both formulations, indicating an almost complete encapsulation. The high EE achieved is probably linked to the high SVT distribution coefficient (log D) of 4.72, which confirms its great affinity for the lipophilic phase and concentration in the core of the nanocapsules [55]. Laser diffraction (LD) analysis showed D[4,3] of 150 ± 7 nm ($LNC_{LMWchit}$), 157 ± 6 nm ($LNC_{HMWchit}$), 163 ± 2 nm ($LNC_{SVT\text{-}LMWchit}$), and 161 ± 3 nm ($LNC_{SVT\text{-}HMWchit}$) with Span values of 1.273 ± 0.085, 1.295 ± 0.101, 1.386 ± 0.028 and 1.209 ± 0.152, respectively. According to the results obtained with this technique, there were no significant difference in terms of particle diameter and polydispersity between the formulations with and without SVT ($p>0.05$). The shape of the curves in the radar chart presented in Figure 1 are fingerprint of the formulations that demonstrate narrow size distributions and confirming the low polydispersity [56]. All the formulations showed similar behaviour and had $d_{0.9}$ calculated both on the cumulative distribution by number and by volume lower than 300 nm (Figure 1).

Preprints (www.preprints.org) | NOT PEER-REVIEWED | Posted: 4 February 2019 doi:10.20944/preprints201902.0034.v1

Peer-reviewed version available at Pharmaceutics 2019, 11, 86; doi:10.3390/pharmaceutics11020086

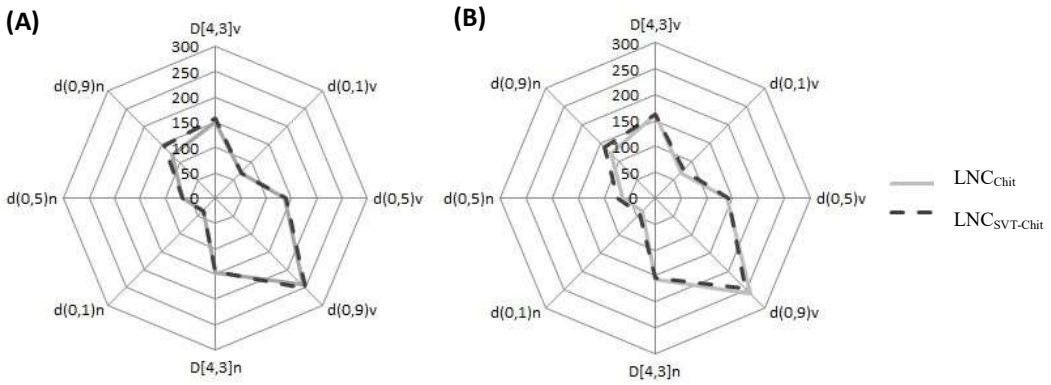

Figure 1. Radar chart presenting the volume-weighted mean diameters (D[4,3]) and the diameters at percentiles 10, 50 and 90 under the size distribution curves by volume and by number of particles. Chitosan-coated simvastatin-loaded lipid-core nanocapsules developed with (a) low MW chitosan and (b) high MW chitosan.

Mean particle size was further confirmed by DLS and NTA analysis as shown in Table 1. DLS analysis showed a narrow particle size distribution for all the formulations (PDI < 0.2). In particular, the encapsulation of SVT did not affect the particle size of nanocapsules coated with low MW chitosan. In fact the diameter of $LNC_{LMWchit}$ and $LNC_{SVT\text{-}LMWchit}$ was not significantly different ($p>0.05$). On the other hand, the presence of SVT led to a significant size increase ($p\leq0.05$) in the case of $LNC_{SVT\text{-}HMWchit}$ (210 ± 10 nm) when compared with blank nanocapsules ($LNC_{HMWchit}$, 188 ± 7 nmm) in the case of NTA analysis, but not in the case of DLS data. This difference may be explained with the formation of a small number of particle agglomerates, compared to the formulation prepared without drug. In addition, these agglomerates appeared to be detected more efficiently by the NTA technique compared to DLS. This is supported by the particle number density (PND) also measured by NTA that evidenced upon SVT encapsulation almost an halving of the particle number density (PND), which was $1.05 \pm 0.36 \times 10^{12}$ particles/mL for $LNC_{HMWchit}$ and $6.60 \pm 0.21 \times 10^{11}$ particles/mL for $LNC_{SVT\text{-}HMWchit}$ (Table 1). Furthermore, in general the nanocapsules coated with HMW chitosan showed a slightly higher mean diameter than those coated with LMW chitosan ($p>0.05$), probably as a consequence of the chitosan higher molecular weight and higher viscosity in the water phase. In general, it has been reported that the higher is the viscosity of the dispersion medium, the higher is the mean diameter of nanoparticles produced [57].

Table 1. Physicochemical characterization of the nanocapsules (n = 3, Mean ± Standard Deviation).

	DLS		NTA			
	Z-average (nm)	PDI	Mean (nm)	PND (particles/mL)	Zeta potential (mV)	pH
$LNC_{LMWchit}$	166 ± 5	0.134 ± 0.017	174 ± 5	$1.29 \pm 0.25 \times 10^{12}$	25.4 ± 4.1	4.09 ± 0.01
$LNC_{SVT\text{-}LMWchit}$	168 ± 5	0.116 ± 0.036	166 ± 7	$1.20 \pm 0.55 \times 10^{12}$	28.95 ± 2.1	4.11 ± 0.02
$LNC_{HMWchit}$	179 ± 14	0.134 ± 0.021	188 ± 7	$1.05 \pm 0.36 \times 10^{12}$	33.6 ± 3.9	4.12 ± 0.03
$LNC_{SVT\text{-}HMWchit}$	185 ± 7	0.164 ± 0.029	210 ± 10	$6.60 \pm 0.21 \times 10^{11}$	33.8 ± 5.5	4.39 ± 0.04

Zeta potential represents the surface charge of particles, and, as expected, the formulations produced with chitosan exhibited a positive zeta potential at the pH of the formulations that was between pH 4.0 and 4.5. In fact, the nanocapsules suspensions showed mildly acid pH values, as

Peer-reviewed version available at Pharmaceutics 2019, 11, 86; doi:10.3390/pharmaceutics11020086

expected due to the use of 1% acetic acid aqueous solution to dissolve chitosan [43]. The zeta potential of $LNC_{LMWchit}$ and $LNC_{HMWchit}$ were similar to those determined for the SVT-loaded nanocapsules. Therefore, the encapsulation of SVT did not significantly affect this parameter ($p>0.05$). The pH value at which the nanoparticles do not exhibit any net charge is termed isoelectric point (IEP). $LNC_{SVT\text{-}LMWchit}$ and $LNC_{SVT\text{-}HMWchit}$ showed their isoelectric point (IEP) at pH value 7.05 ± 0.19 and 7.17 ± 0.45, respectively. The positive zeta potential obtained for all formulations prepared and the IEP near to IEP of chitosan (IEP=6.8) [58] are good indicatives that the chitosan is present at the external interface of the nanocapsules. $LNC_{SVT\text{-}LMWchit}$ and $LNC_{SVT\text{-}HMWchit}$ were further characterized in terms of the morphology (Figure 2).

Concerning nanocapsules morphology, TEM images clearly display spherical-shaped particles, with a core with low electron density, as expected for lipid nanocapsules. Also form the point of view of particle diameter the images are in good agreement with the mean nanocapsule size determined with DLS, NTA and LD.

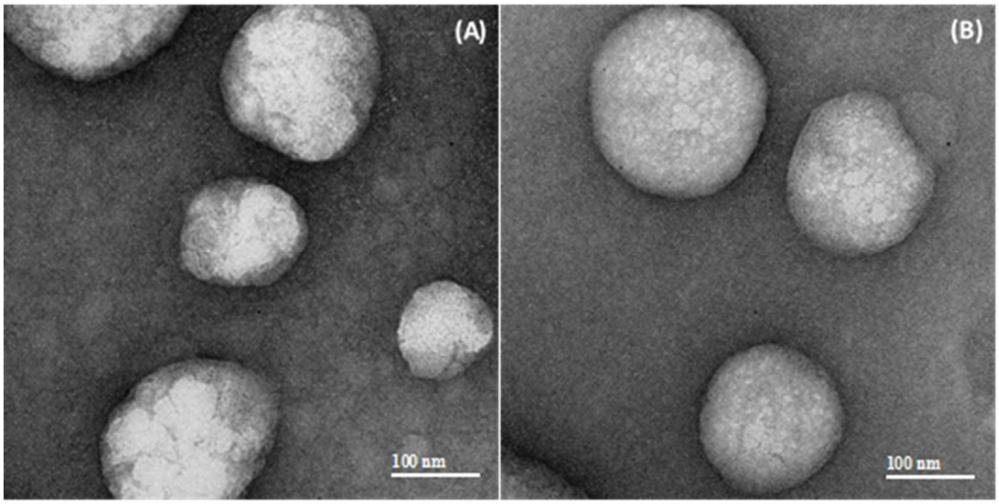

Figure 2. Transmission electron microscopy (TEM) micrographs (magnification 40,000×) of chitosan-coated lipid core nanocapsules: (A) $LNC_{SVT\text{-}LMWchit}$ and (B) $LNC_{SVT\text{-}HMWchit}$.

3.2 Mucoadhesion studies

To investigate the interaction between the formulations and mucin, a mucoadhesion index (MI), the PDI and zeta potential of mixtures between the nanocapsules and mucin were determined for different mucin weight ratios f (Figure 3). For $LNC_{SVT\text{-}LMWchit}$ in the range of f values up to 0.3, particle size and MI values increased to a maximum 474 ± 6 nm and 2.87 ± 0.07 (f = 0.3), respectively. Similarly, $LNC_{SVT\text{-}HMWchit}$ particle size and MI increased in the f range from 0 to 0.55, reaching a maximum of 557 ± 30 nm, 3.01 ± 0.28 (f = 0.55), respectively (Figure 3a). Despite the increase of the fraction by weight of mucin above f values of 0.3, for $LNC_{SVT\text{-}LMWchit}$ particle size and MI decreased to 318 ± 5 nm and 1.93 ± 0.04 for f values of 0.85. It has been hypothesized here, that while at values of f around 0.3 nanocapsules are able to form large agglomerates with mucin chains entangled and linked with more nanoparticles, above this value the mucin is in such a large excess that almost single particles are enrobed with mucins leading to a decrease in the overall mean particle size. In fact, the MI values for f 0.55 and 0.85 do not change significantly. On the other hand, for $LNC_{SVT\text{-}HMWchit}$ this decrease in the MI occurs only for f values above 0.55, with particle size and MI decreasing to 321 ± 7 nm, 1.73 ± 0.08 (f = 0.85). Therefore, the MI maximum was observed at lower f values (0.3) for $LNC_{SVT\text{-}LMWchit}$ and higher f values (0.55) for $LNC_{SVT\text{-}HMWchit}$, indicating a higher capacity to interact with larger quantities of mucin for nanoparticles coated with high MW chitosan, macroscopically translated in a more efficient mucoadhesion.

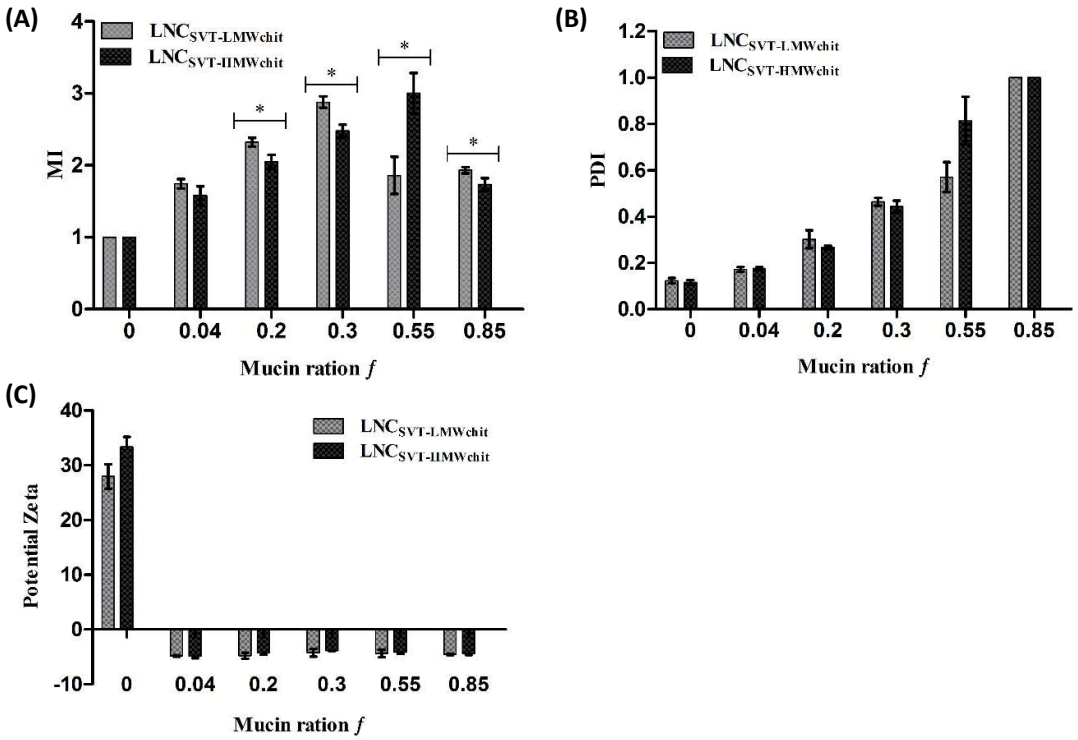

Figure 3. (A) Mucoadhesive index (MI) values, (B) PDI and (C) Zeta potential measured for various mixtures of mucin and nanocapsules. Values of the two formulations were obtained before (f = 0) and after incubation with different mucin weight ratios f.

The polydispersity index (PDI) before nanocapsules interaction with mucin was 0.12 ± 0.01 for $LNC_{SVT\text{-}LMWchit}$ and 0.11 ± 0.01 for $LNC_{SVT\text{-}HMWchit}$. After mixing the nanocapsules with mucin, PDI progressively increased for both formulations up to 1 (f = 0.85), indicating the formation of agglomerates and the switch to highly polydisperse particle size distribution (Figure 3b). The zeta potential of the formulations that was initially positive due to the chitosan coating, immediately after interaction even with the smallest amount of mucin (f = 0.04) became negative for both formulations (-4.79 ± 0.12 mV for $LNC_{SVT\text{-}LMWchit}$ and -4.83 ± 0.67 mV for $LNC_{SVT\text{-}HMWchit}$) and remained roughly constant for both formulations even increasing f values (Figure 3c).

3.3 In Vitro Drug Release

The *in vitro* release profile of simvastatin-loaded chitosan coated lipid core nanocapsules were performed over 8 hours (Figure 4). A solution of simvastatin was used as control. It can be observed that 56.25 ± 2.48% of SVT diffused out from the dialysis bag when using the control simvastatin solution within 8 hours. On the other hand, the drug released from $LNC_{SVT\text{-}LMWchit}$ and $LNC_{SVT\text{-}HMWchit}$ after 8 hours was 37.23 ± 1.50% and 30.98 ± 1.13%, respectively. These results show that nanocapsules provided a controlled release of simvastatin and that the different type of chitosan affected the drug release rate. Indeed, the release of SVT from $LNC_{SVT\text{-}HMWchit}$ was slower in comparison to the $LNC_{SVT\text{-}LMWchit}$.

Preprints (www.preprints.org) | NOT PEER-REVIEWED | Posted: 4 February 2019 doi:10.20944/preprints201902.0034.v1

Peer-reviewed version available at Pharmaceutics 2019, 11, 86; doi:10.3390/pharmaceutics11020086

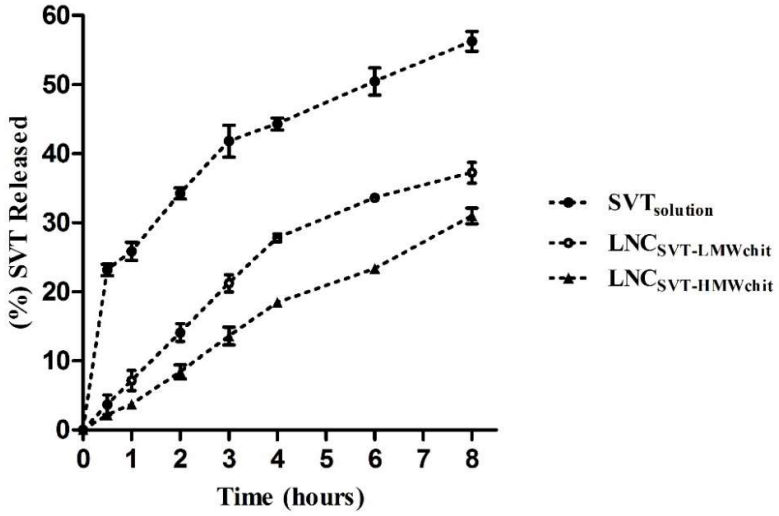

Figure 4. In vitro drug release profile from LNCSVT-LMWchit, LNCSVT-HMWchit and from control (SVT solution) using the dialysis bag method at 37 °C (n = 3, ± SD).

3.4 Transport Studies on a Nasal Cell Model

To confirm the potential permeability enhancement effects of the nanocapsules, the total amount of SVT transported across nasal mucosa model was determined using RPMI2650 human nasal epithelial cells [52]. Figure 5 shows the amount of SVT transported using the formulations compared to a suspension of the raw material over 4 hours. After 1 h of the experiment, the formulations already showed increased permeation compared to the control. However, no significant differences ($p>0.05$) were observed at 1 hour for the SVT permeation between LNCSVT-LMWchit to LNCSVT-HMWchit. After the first hour however, each single time point showed an amount of SVT transported to be statistically different between the formulations ($p < 0.05$) and confirming the greater permeation of LNCSVT-LMWchit.

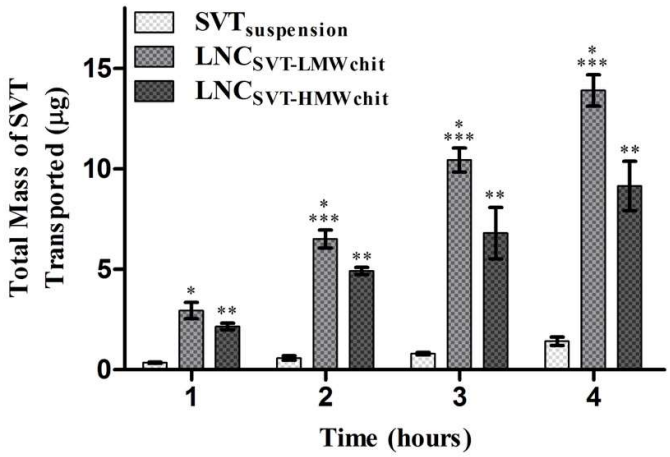

Figure 5. Amount (µg) of SVT transported across RPMI 2650 cells grown under air-liquid interface conditions (n = 4, ± SD). Significant difference ($p<0.05$) is expressed considering the following comparisons: ∗SVT *versus* LNCSVT-LMWchit, ∗∗SVT *versus* LNCSVT-HMWchit *** LNCSVT-LMWchit *versus* LNCSVT-HMWchit.

3.5 Ex vivo Transport Experiments across Rabbit Nasal Mucosa

Figure 6a shows the SVT permeation across excised rabbit nasal mucosa using Franz type vertical diffusion cells. The results of *ex vivo* permeation studies on rabbit nasal mucosa evidenced that the formulations significantly increased the permeation of SVT compared to control. The $LNC_{SVT\text{-}LMWchit}$ showed the highest percent SVT permeation after 4 h (19.16 ± 0.53%·cm^{-2}), followed by $LNC_{SVT\text{-}HMWchit}$ (10.99 ± 0.53%·cm^{-2}), while the control (SVT suspension) showed an extremely low permeation (2.60 ± 0.21%·cm^{-2}). The results indicate that SVT permeation from $LNC_{SVT\text{-}LMWchit}$ was 1.74 and 7.4 times greater than $LNC_{SVT\text{-}HMWchit}$ and SVT control, respectively.

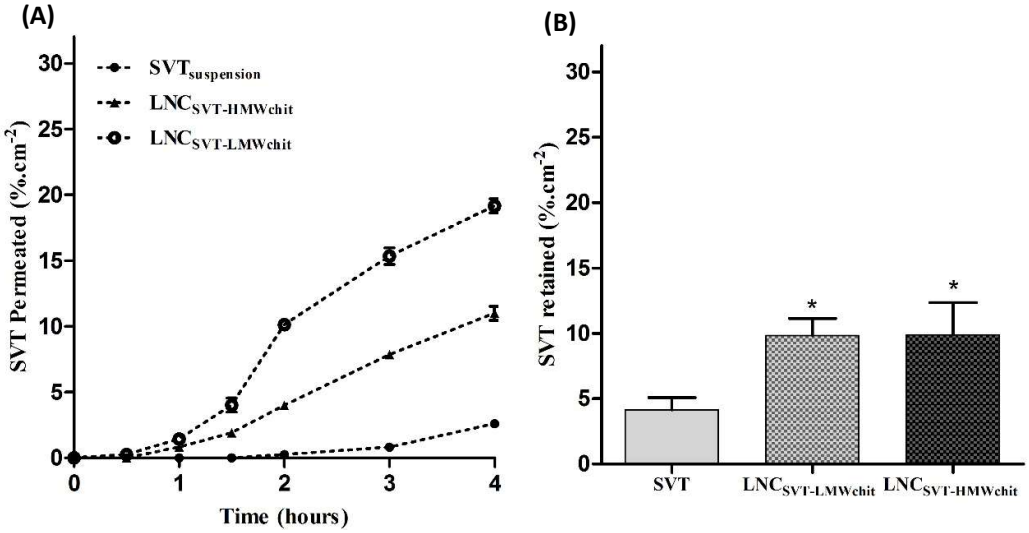

Figure 6. (A) *Ex vivo* SVT permeation across rabbit nasal mucosa until 4 h in simulated nasal electrolytic solution (SNES) containing 0.5% of polysorbate 80 at 37 °C (n = 3, ± SD). (B) Percentage of SVT retained in nasal mucosa after 4 h of permeation test in Franz-type diffusion cell (n = 3, ± SD). Asterisk (*) indicates significant difference between SVT control *versus* $LNC_{SVT\text{-}LMWchit}$ and $LNC_{SVT\text{-}HMWchit}$.

The results of SVT retained in the mucosa tissue after 4h of experiment are shown in Figure 6b. It can be seen that there was better retention of both formulations with respect to the control. The SVT fraction found in the tissue for the control was 4.16 ± 0.92 %·cm^{-2}, while in the case of $LNC_{SVT\text{-}LMWchit}$ and $LNC_{SVT\text{-}HMWchit}$ the fraction of simvastatin found in the tissue was more than doubled, i.e. 9.83 ± 1.31 and 9.88 ± 2.47%·cm^{-2}, respectively. In this case, the difference between the amount of retained SVT from $LNC_{SVT\text{-}LMWchit}$ and $LNC_{SVT\text{-}HMWchit}$ was not statistically significant.

3.6 Preliminary nasal toxicity studies

Nasal mucosa histopathology studies were performed to assess the integrity of rabbit mucosa after 4h of the permeation test. As shown in Figure 7, the mucosa treated with PBS pH 6.4 (negative control), SVT, $LNC_{SVT\text{-}LMWchit}$ and $LNC_{SVT\text{-}HMWchit}$ did not show any evident structural damage. The results from histological examinations indicate that LNC nanocapsules do not cause any irritation or toxicity and can be considered to be biocompatible for nasal administration.

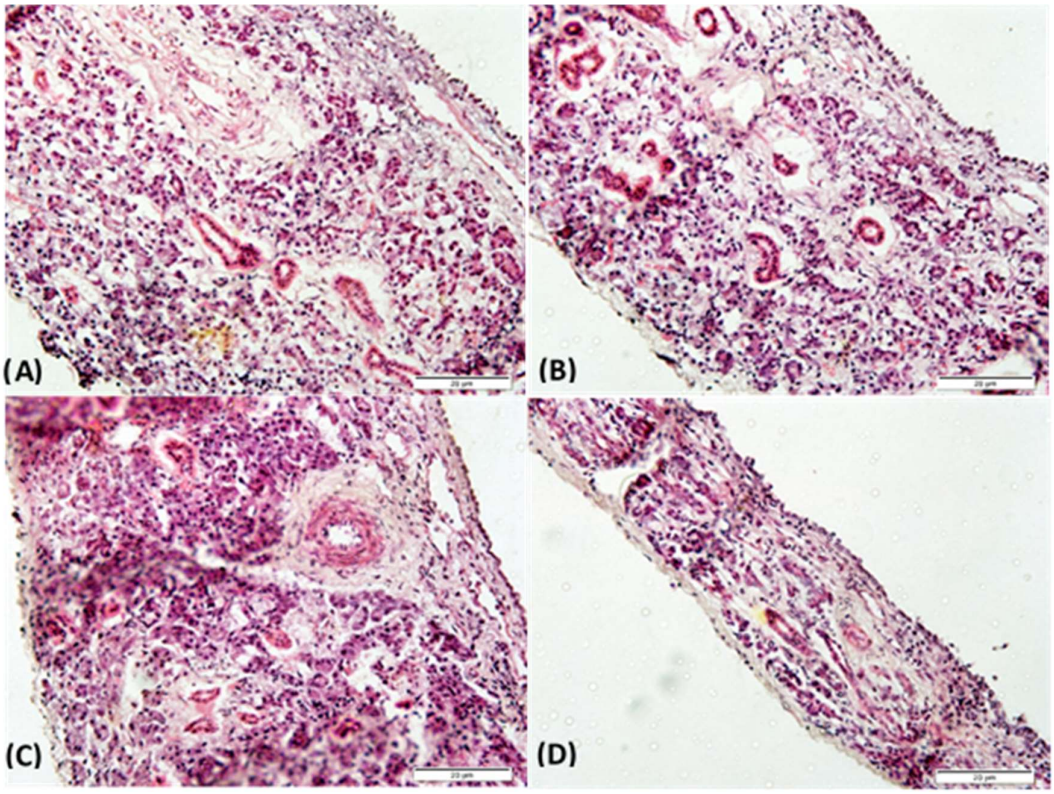

Figure 7. Histopathological sections of rabbit nasal mucosa after 4 h of permeation test in Franz-type diffusion cell treated with (A) PBS pH 6.4 (negative control), (B) SVT, (C) $LNC_{SVT\text{-}LMWchit}$ and (D) $LNC_{SVT\text{-}HMWchit}$. Stained with hematoxylin and eosin.

4. Discussion

Over the past couple of decades pharmaceutical nanotechnology have received considerable attention and demonstrated significant potential for the development of innovative medicinal products both for the therapy and the diagnosis of severe diseases [59]. In this work, we report a new preparation method of lipid-core PCL nanocapsules, optimizing a two-step process (self-assembly step followed by a coating step) into a one-pot technique to develop chitosan-coated nanoparticles. Moreover, we compared the pharmaceutically relevant properties in terms of physicochemical characterization, mucoadhesive properties, drug release and permeability studies of $LNC_{SVT\text{-}LMWchit}$ and $LNC_{SVT\text{-}HMWchit}$ coated by chitosan with low MW and high MW in view of a nose-to-brain administration.

Polymeric nanocapsules containing poly (ε-caprolactone), capric/caprylic triglyceride, sorbitan monostearate and coated with chitosan were developed. This formulation has the advantage of encapsulating efficiently a lipophilic drug as simvastatin [34,35]. The combination between this composition and the interfacial deposition of pre-formed polymer method produced nanocapsules with adequate particle size and narrow size distributions as was confirmed by complementary techniques such as laser diffraction, DLS and NTA. Besides that, coating the nanocapsules with chitosan with different molecular weight (21 KDa and 152 KDa) influenced their pharmaceutical properties. For example, chitosan molecular weight and viscosity in water affected the size of the nanoparticles. In fact, particle size could be reduced by using lower molecular weight chitosan [60,61]. Actually, $LNC_{SVT\text{-}HMWchit}$ higher mean particle hydrodynamic diameter could be attributed to the length chains of chitosan present on the particle surface, possibly expanding the water hydration shell of the nanoparticle. In addition, chitosan low MW has been reported to have higher aqueous solubility and this together with shorter polymer chains contributed to forming smaller particles compared to chitosan high MW [62]. The positive zeta potential obtained for all formulations is an

evidence of the polysaccharide coating. Furthermore, using different chitosan did not cause significant changes in zeta potential of both formulations, probably due of a similar degree of deacetylation (95%) [63]. Mucoadhesive polymers such as chitosan represent a significant strategy to overcome the nasal drug delivery limits as low membrane permeability, short residence time and mucociliary clearance. The polysaccharide presence on nanocapsules surface is expected to prolong permanence of the formulation in the nasal cavity, open the tight junctions between nasal epithelial cells and promote the drug permeation through the biological barriers granting access to the CNS [64,65,66]. For these reasons, the evaluation of the ability of nanocapsules to interact with mucin is of great interest for nasal administration. Mucous membranes internally delimiting the body cavities (stomach, esophagus, cornea, oral cavity, reproductive and respiratory tracts) and are characterized by a superficial mucus layer with protective and lubricating function [67]. The mucus is composed of water (approximately 95%), lipids, inorganic salts and mucin, a glycoprotein composed by N-acetylgalactosamine, N-acetylglucosamine, fucose, galactose, and sialic acid, responsible for the adhesive properties and the viscosity of the mucus [65]. Lipophilic drugs show an affinity for mucus glycoproteins reducing the adsorption and the bioavailability. This issue, together with the drug poor aqueous solubility, are limiting factor for the nose-to-brain delivery of lipophilic drugs. To improve the transport of SVT through this barrier we used nanoparticles as a drug delivery system [68].

Our results showed how, for both formulations, particle size and MI increased with the increase in the mucin weight ratio until a critical point. A previous study [50] has led to the conclusion that the nanoparticles in mucin solution form agglomerates in which the nanoparticles are the points of contact between negatively charged mucin chains. Beyond the critical value of the mucin ratio the repulsive forces among the mucin chains break these agglomerates. Our results support this theory, nevertheless it has to be stressed that the decrease of MI observed for high mucin weight ratio does not indicate a decrease in the mucoadhesive capacity of the formulations [50]. However, the results indicate how in mucin excess, the smaller aggregates are formed in order to minimize the repulsive forces between the chains of the mucin and maximize the points of contact between the positive charges of chitosan and the negative mucin chains. Moreover, it was noticed that the critical point of the formulations was different for the nanocapsules coated with chitosan with different characteristics ($LNC_{SVT\text{-}LMWchit}$ $f = 0.3$ and for $LNC_{SVT\text{-}HMWchit}$ $f = 0.55$). This difference could be attributed to the different chain lengths of the two chitosan batches [62]. Indeed, in a previous study conducted with a different method Menchicchi and co-authors proposed that mucin interact mostly with high molecular weight chitosan [69]. On the other hand, the results presented in this paper compared to similar uncoated LNC demonstrate a large increase in the mucoadhesive capacity due to the presence of chitosan. The uncoated LNC showed values of MI = 1.36, PDI = 0.51 and zeta potential of -9.54 mV after contact with the maximum concentration of mucin (0.5% w/v) [70]. The PDI increase with the increase in the f mucin ratio corroborates the above-mentioned explanation. In fact, PDI results indicated that the heterogeneity of the distribution of the particle size in solution increased along with the mucin weight ratio because of the formation of aggregates of different sizes. The oligosaccharide chains of mucin glycoproteins present terminal sialic acid residues confer negative charge to the molecule, therefore the variation of the particle zeta potential from positive to negative values demonstrates how the mucin enrobes nanocapsules interacting with their surface layer of chitosan. This suggests that the mucoadhesion mechanism are driven by electrostatic interaction of positively charged amine groups of D-glucosamine molecules of chitosan with negatively charged sialic acid residues of mucin [71].

SVT-loaded lipid core nanocapsules formulation was able to control the drug release due the two diffusional barriers: the PCL polymer wall and the lipid dispersion present in the nanocapsule core. The nanoencapsulation reduced the diffusion rate of SVT across a dialysis membrane, confirming data frequently described in the literature as a property of polymeric nanoparticles [33]. Regarding the comparison between the two formulations, $LNC_{SVT\text{-}HMWchit}$ afforded better control of drug release. In order to explain the different release profile, we evaluated the differences in terms of physicochemical properties. Firstly, this can be explained due to the higher viscosity of the chitosan used to develop the $LNC_{SVT\text{-}HMWchit}$. Previous studies demonstrated that the viscosity of the chitosan

is an important factor for modulating the release control [72]. Moreover, nanoparticle size can influence in the release profile, which increases with decreasing particle size. Indeed, $LNC_{SVT\text{-}LMWchit}$ had lower mean particle diameter than $LNC_{SVT\text{-}HMWchit}$, that could contribute to explain the different release profile between them because of the greater available surface area [73,74]

The permeation across RPMI 2650 human nasal cell line showed that the SVT transported across the nasal cell model by $LNC_{SVT\text{-}LMWchit}$ and $LNC_{SVT\text{-}HMWchit}$ can enhance the drug transport across a cell pseudo-monolayer that also secrete mucin on its apical surface. The increase of SVT permeation across the human nasal cell layer can be explained by different mechanisms. In literature, chitosan is associated with an opening of tight junctions that increase cell layers permeability. However, this mechanism is generally favoring the permeation of water-soluble drugs and it has been evidenced that is slightly less efficient for chitosan bound to nanoparticles compared to simple polysaccharide solutions [75]. More recently, it has been demonstrated that the biodegradation of nanocapsules by enzymes in the mucus barrier or intracellularly could be pivotal in enhancing transcellular transport of lipophilic drugs [76]. The results of the *ex vivo* permeation studies on rabbit nasal mucosa confirmed and further added evidence of the fact that the nanoencapsulation of SVT significantly increased its permeation across excised nasal mucosa. In this case, the higher permeation evidenced for $LNC_{SVT\text{-}LMWchit}$ could be explained by a combination of factors. The smaller particle size of nanocapsules coated with low molecular weight chitosan could have facilitated the absorption to the mucosal tissue as reported before [77]. Moreover, an important factor is the bioadhesion of the nanostructures, as previously explained given by the particles shell of chitosan that interacts by electrostatic forces with the anionic sites of the nasal mucus [64]. However, from the mucoadhesion data a better interaction with mucus could be expected from nanocapsules coated with the high molecular weight chitosan. However, the slower release kinetics evidenced for these particles have probably contributed to limit the amount of drug permeated, especially considering that drug accumulation into the tissue is superimposable for the two nanocapsules formulations.

Previous findings [78,79], agreed that chitosan coated nanoparticles increased the drug permeation across the nasal mucosa compared to the free drug control. This controlled SVT permeation, together with mucoadhesion effect, may be an important strategy to prolong the effect of the drug when administered via the nasal route.

5. Conclusions

In the present investigation, the coating process of lipid-core nanocapsules using a one-pot technique approach was presented. Furthermore, two chitosan-coated simvastatin-loaded lipid core nanocapsules suitable for nasal administration were successfully developed. Both the nanoparticles produced with different chitosan were designed to have adequate physicochemical and mucoadhesive properties for a potential nose-to-brain application. The formulations prepared combine a controlled release of simvastatin and mucoadhesion properties able to increase the drug permeation across the nasal mucosa, as demonstrated using two different model of nasal epithelium. In summary, simvastatin-loaded chitosan-coated lipid core nanocapsules seems to be a promising mucoadhesive system for nose-to-brain delivery of poorly soluble anticancer drugs. The follow up studies will focus on the investigation of the potential of these nanoparticles for the treatment of brain tumors involving studies with glioma cells and an orthotopic intracranial tumor model in mice.

Author Contributions: Conceptualization, A.R.P. S.S.G., and F.S.; Methodology, F.A.B., S.P., T.A., G.D.S., G.G.P., M.M., L.T.F.; Investigation, F.A.B., S.P.; Resources, A.R.P., S.S.G.; Writing-Original Draft Preparation, F.A.B., S.P.; Writing-Review & Editing, F.A.B., F.S.; Supervision, A.B., G.C., F.S.

Acknowledgments: Franciele Aline Bruinsmann, Fabio Sonvico, Adriana Raffin Pohlmann, and Silvia Stanisçuaski Guterres would like to acknowledge the Brazilian government as recipients of CNPq grants in the programs "Ciências sem Fronteiras" (BOLSA PESQUISADOR VISITANTE ESPECIAL—PVE 401196/2014-3) and "Produtividade em Pesquisa". This study was financed in part by the Coordenação de Aperfeiçoamento de Pessoal de Nível Superior – Brasil (CAPES) – Finance Code 001.

Conflicts of Interest: The authors declare no conflict of interest.

References

1. Chiang, K.H.; Cheng, W.L.; Shih, C.M.; Lin, Y.W.; Tsao, N.W.; Kao, Y.T.; Lin, C.T.; Wu, S.C.; Huang, C.Y.; Lin, F.Y. Statins, HMG-CoA Reductase Inhibitors, Improve Neovascularization by Increasing the Expression Density of CXCR4 in Endothelial Progenitor Cells. *PLoS One* **2015**, 10(8), e0136405.
2. Liao, J.K.; Ulrich, L. Pleiotropic effects of statins. Annu. *Rev. Pharmacol. Toxicol.* **2005**, 45, 89-118.
3. Davies, J.T.; Delfino, S.F.; Feinberg, C.E.; Johnson, M.F.; Nappi, V.L.; Olinger, J.T.; Schwab, A.P.; Swanson, H.I. Current and Emerging Uses of Statins in Clinical Therapeutics: A Review. *Lipid Insights* **2016**, 9, 13-29.
4. Jain, M.K.; Ridker, P.M. Anti-inflammatory effects of statins: clinical evidence and basic mechanisms. *Nat. Rev. Drug Discov*. **2005**, 4, 977-987.
5. Liao, K.J. Isoprenoids as mediators of the biological effects of statins. *J. Clin. Invest*. **2002**, 110, 285–288.
6. Tanaka, S.; Fukumoto, Y.; Nochioka, K.; Minami, T.; Kudo, S.; Shiba, N.; Shimokawa, H. Statins exert the pleiotropic effects through small GTP-binding protein dissociation stimulator upregulation with a resultant Rac1 degradation. *Arter. Thromb. Vasc. Biol*. **2013**, 33, 1591-1600.
7. Hindler, K.; Cleeland, C.S.; Rivera, E.; Collard, C.D. The role of statins in cancer therapy. *Oncologist.* **2006**, 11, 306-315.
8. Altwairgi, A.K. Statins are potential anticancerous agents (Review). *Oncol. Rep.* **2015**, 33, 1019-1039.
9. Gazzerro, P.; Proto, M.C.; Gangemi, G.; Malfitano, A.M.; Ciaglia, E.; Pisanti, S.; Santoro, A.; Laezza, C.; Bifulco, M. Pharmacological actions of statins: a critical appraisal in the management of cancer. *Pharmacol. Rev.* **2012**, 64, 102-146.
10. Wejde J., Hjertman, M.; Carlberg, M.; Egestad, B.; Griffiths, W.J.; Sjövall, J.; Larsson, O. Dolichol-like lipids with stimulatory effect on DNA synthesis: substrates for protein dolichylation. *J. Cell Biochem*. **1998**, 71, 502-514.
11. Bifulco, M. Therapeutic potential of statins in thyroid proliferative disease. *Nat. Clin Pract. Endocrinol. Metab.* **2008**, 4, 242-243.
12. Chan, K.K.; Oza, A.M.; Siu, L.L. The statins as anticancer agents. *Clin. Cancer Res*. **2003**, 9, 10-19.
13. Frick, M.; Dulak, J.; Cisowski, J.; Jozkowicz, A.; Zwick, R.; Alber, H.; Dichtl, W.; Schwarzacher, S.P.; Pachinger, O.; Weidinger, F. Statins differentially regulate vascular endothelial growth factor synthesis in endothelial and vascular smooth muscle cells. *Atherosclerosis* **2003**, 170, 229-236.
14. Denoyelle, C.; Vasse, M.; Körner, M.; Mishal, Z.; Ganné, F.; Vannier, J.P.; Soria, J.; Soria, C. Cerivastatin, an inhibitor of HMG-CoA reductase, inhibits the signaling pathways involved in the invasiveness and metastatic properties of highly invasive breast cancer cell lines: an in vitro study. *Carcinogenesis* **2001**, 1139-1148.
15. Yanae, M.; Tsubaki, M.; Satou, T.; Itoh, T.; Imano, M.; Yamazoe, Y.; Nishida, S. Statin-induced apoptosis via the suppression of ERK1/2 and Akt activation by inhibition of the geranylgeranyl-pyrophosphate biosynthesis in glioblastoma. *J. Exp. Clin. Cancer Res*. **2011**, 30, 74.
16. Wu, H.; Jiang, H.; Lu, D.; Xiong, Y.; Qu, C.; Zhou, D.; Mahmood, A.; Chopp, M. Effect of simvastatin on glioma cell proliferation, migration, and apoptosis. *Neurosurgery* **2009**, 65, 1087-1096.
17. Bababeygy, S.R.; Polevaya, N.V.; Youssef, S.; Sun, A.; Xiong, A.; Prugpichailers, T.; Veeravagu, A.; Hou, L.C.; Steinman, L.; Tse, V. HMG-CoA Reductase Inhibition Causes Increased Necrosis and Apoptosis in an In Vivo Mouse Glioblastoma Multiforme Model. *Anticancer Res.* **2009**, 29, 4901-4908.
18. Parrish, K.E.; Sarkaria, J.N.; Elmquist, W.F. Improving drug delivery to primary and metastatic brain tumors: strategies to overcome the blood-brain barrier. *Clin. Pharmacol. Ther*. **2015**, 97, 336-346.
19. Romana, B.; Batger, M.; Prestidge, C.A.; Colombo, G.; Sonvico, F. Expanding the therapeutic potential of statins by means of nanotechnology enabled drug delivery systems. *Curr. Top Med. Chem*. **2014**, 14, 1182-1193.
20. Mittal, D.; Ali, A.; Md, S.; Baboota, S.; Sahni, J.K.; Ali, J. Insights into direct nose to brain delivery: current status and future perspective. *Drug Deliv*. **2014**, 21, 75-86.
21. Sonvico, F.; Clementino, A.; Buttini, F.; Colombo, G.; Pescina, S.; Guterres, S.S.; Pohlmann, A.R.; Nicoli, S. Surface-Modified Nanocarriers for Nose-to-Brain Delivery: From Bioadhesion to Targeting. *Pharmaceutics* **2018**, 10, 34.
22. Bernardi A.; Braganhol, E.; Jäger, E.; Figueiró, F.; Edelweiss, M.I.; Pohlmann, A.R.; Guterres, S.S.; Battastini, A.M. Indomethacin-loaded nanocapsules treatment reduces in vivo glioblastoma growth in a rat glioma model. *Cancer Lett*. **2009**, 281, 53-63.

23. Patel, T.; Zhou, J.; Piepmeier, J.M.; Saltzman. W.M. Polymeric Nanoparticles for Drug Delivery to the Central Nervous System. *Adv. Drug Deliv. Rev*. **2012**, 64, 701-705.
24. Rodrigues, S.F.; Fiel, L.A.; Shimada, A.L.; Pereira, N.R.; Guterres, S.S.; Pohlmann, A.R.; Farsky, S.H. Lipid-Core Nanocapsules Act as a Drug Shuttle Through the Blood Brain Barrier and Reduce Glioblastoma After Intravenous or Oral Administration. *J. Biomed. Nanotechnol*. **2016**, 12, 986-1000.
25. Bahadur, S.; Pathak, K. Physicochemical and physiological considerations for efficient nose-to-brain targeting. *Expert Opin. Drug Deliv*. **2012**, 9, 19-31.
26. Comfort, C.; Garrastazu, G.; Pozzoli, M.; Sonvico, F. Opportunities and challenges for the nasal administration of nanoemulsions. *Curr. Top Med. Chem*. **2015**, 15, 356-368.
27. Illum, L. Nasal drug delivery-possibilities, problems and solutions. *J. Control. Release* **2003**, 87, 187-198.
28. Prego, C.; Torres, D.; Alonso, M.J. Chitosan nanocapsules: a new carrier for nasal peptide delivery. *J. Nanosci. Nanotechnol*. **2006**, 6, 2921-2928.
29. Fonseca, F.N.; Betti, A.H.; Carvalho, F.C.; Gremião, M.P.; Dimer, F.A.; Guterres, S.S.; Tebaldi, M.L.; Rates, S.M.; Pohlmann, A.R. Mucoadhesive Amphiphilic Methacrylic Copolymer-Functionalized Poly(ε-caprolactone) Nanocapsules for Nose-to-Brain Delivery of Olanzapine. *Biomed Nanotechnol.* **2015**, 11, 1472-1481.
30. Clementino, A.; Batger, M.; Garrastazu, G.; Pozzoli, M.; Del Favero, E.; Rondelli, V.; Gutfilen, B.; Barboza, T.; Sukkar, M.B.; Souza, S.A.; Cantù. L.; Sonvico, F. The nasal delivery of nanoencapsulated statins – an approach for brain delivery. *Int J Nanomedicine* **2016**, 11, 6575–6590.
31. Couvreur, P.; Barratt, G.; Fattal, E.; Vauthier, C. Nanocapsule Technology: A Review. *Crit. Rev. Ther. Drug Carrier Syst*. **2002**, 19, 99-134.
32. Mora-Huertas, C.E.; Fessi, H.; Elaissari, A. Polymer-based nanocapsules for drug delivery. *Int. J. Pharm*. **2010**, 385, 113-142.
33. Pohlmann, A.R.; Fonseca, F.N.; Paese, K.; Detoni, C.B.; Coradini, K.; Beck, R.C.; Guterres, S.S. Poly (e-caprolactone) microcapsules and nanocapsules in drug delivery. *Expert Opin. Drug Deliv*. **2013**, 10, 623-638.
34. Jäger, E.; Venturini, C.G.; Poletto, F.S.; Colomé, L.M.; Pohlmann, J.P.; Bernardi, A.; Battastini, A.M.; Guterres, S.S.; Pohlmann, A.R.. Sustained release from lipid-core nanocapsules by varying the core viscosity and the particle surface area. *J. Biomed. Nanotechnol*. **2009**, 5, 130-140.
35. Venturini, C.G.; Jäger, E.; Oliveira, C.P.; Bernardi, A.; Battastini, A.M.O.; Guterres, S.S.; Pohlmann, A.R. Formulation of lipid core nanocapsules. *Colloids Surf. A. Physicochem. Eng. Asp*. **2011**, 375, 200-208.
36. Fiel, L.A.; Rebêlo, L.M.; Santiago, T.M.; Adorne, M.D.; Guterres, S.S.; Sousa, J.S.; Pohlmann, A.R. Diverse Deformation Properties of Polymeric Nanocapsules and Lipid-Core Nanocapsules. *Soft Matter* **2011**, 7, 7240-7247.
37. Frozza, R.L.; Bernardi, A.; Paese, K.; Hoppe, J.B.; da Silva, T.; Battastini, A.M.; Pohlmann, A.R.; Guterres, S.S.; Salbego, C. Characterization of trans-resveratrol-loaded lipid-core nanocapsules and tissue distribution studies in rats. *J. Biomed. Nanotechnol*. **2010**, 6, 694-703.
38. Zanotto-Filho A.; Coradini, K.; Braganhol, E.; Schröder, R.; de Oliveira, C.M.; Simões-Pires, A.; Battastini, A.M.; Pohlmann, A.R.; Guterres, S.S.; Forcelini, C.M.; Beck, R.C.; Moreira, J,C. Curcumin-loaded lipid-core nanocapsules as a strategy to improve pharmacological efficacy of curcumin in glioma treatment. *Eur. J. Pharm. Biopharm*. **2013**, 83, 156-167.
39. Dimer, F.A.; Ortiz, M.; Pase, C.S.; Roversi, K.; Friedrich, R.B.; Pohlmann, A.R.; Burger, M.E.; Guterres, S.S. Nanoencapsulation of Olanzapine Increases Its Efficacy in Antipsychotic Treatment and Reduces Adverse Effects. *J. Biomed. Nanotechnol*. **2014**, 10, 1137-1145.
40. Figueiró, F.; Bernardi, A.; Frozza, R.L.; Terroso, T.; Zanotto-Filho, A.; Jandrey, E.H.; Moreira, J.C.; Salbego, C.G.; Edelweiss, M.I.; Pohlmann, A.R.; Guterres, S.S.; Battastini, A.M. Resveratrol-loaded lipid-core nanocapsules treatment reduces in vitro and in vivo glioma growth. *J. Biomed. Nanotechnol*. **2013**, 9, 516-526.
41. Figueiró, F.; de Oliveira, C.P.; Rockenbach, L.; Mendes, F.B.; Bergamin, L.S.; Jandrey, E.H.; Edelweiss, M.I.; Guterres, S.S.; Pohlmann, A.R.; Battastini, A.M. Pharmacological Improvement and Preclinical Evaluation of Methotrexate-Loaded Lipid-Core Nanocapsules in a Glioblastoma Model. *J. Biomed. Nanotechnol*. **2015**, 11, 1808-1818.
42. Drewes, C.C.; Fiel, L.A.; Bexiga, C.G.; Asbahr, A.C.; Uchiyama, M.K.; Cogliati, B.; Araki, K.; Guterres, S.S.; Pohlmann, A.R.; Farsky, S.P. Novel therapeutic mechanisms determine the effectiveness of lipid-core nanocapsules on melanoma models. *Int. J. Nanomedicine* **2016**, 11, 1261-1279.

43. Bender, E.A.; Adorne, M.D.; Colomé, L.M.; Abdalla, D.S.P.; Guterres, S.S.; Pohlmann, A.R. Hemocompatibility of poly(epsilon-caprolactone) lipid-core nanocapsules stabilized with polysorbate 80-lecithin and uncoated or coated with chitosan. *Int. J. Pharm.* **2012**, 426, 271-279.
44. Muxika, A.; Etxabide, A.; Uranga, J.; Guerrero, P.; De la Caba, K. Chitosan as a bioactive polymer: Processing, properties and applications. *Int. J. Biol. Macromol.* **2017**, 105, 1358-1368.
45. Kim, I.Y.; Seo, S.J.; Moon, H.S.; Yoo, M.K.; Park, I.Y.; Kim, B.C.; Cho, C.S. Chitosan and its derivatives for tissue engineering applications. *Biotechnol. Adv.* **2008**, 26, 1-21.
46. Rodrigues, S.; Dionísio, M.; López, C.R.; Grenha, A. Biocompatibility of Chitosan Carriers with Application in Drug Delivery. *J. Funct. Biomater.* **2012**, 3, 615-641.
47. Ways, T.M.M; Lau, W.M.; Khutoryanskiy, V.V. Chitosan and Its Derivatives for Application in Mucoadhesive Drug Delivery Systems. *Polymers* **2018**, 10, 267.
48. Ali, A.; Ahmed, S. A review on chitosan and its nanocomposites in drug delivery. *Int. J. Biol. Macromol.* **2018**, 109, 273-286.
49. Bernkop-Schnürch, A.; Dünnhaupt, S. Chitosan-based drug delivery systems. *Eur. J. Pharm. Biopharm.* **2012**, 81. 463-469.
50. Eliyahu, S.; Aharon, A.; Bianco-Peled, H. Acrylated Chitosan Nanoparticles with Enhanced Mucoadhesion. *Polymers* **2018**, 10, 106.
51. Castile, J.; Cheng, Y.H.; Simmons, B.; Perelman, M.; Smith, A.; Watts, P. Development of in vitro models to demonstrate the ability of PecSys®, an in situ nasal gelling technology, to reduce nasal run-off and drip. *Drug Dev. Ind. Pharm.* **2013**, 39, 816-824.
52. Pozzoli, M.; Ong, H.X.; Morgan, L.; Sukkar, M.; Traini, D.; Young, P.M.; Sonvico, F. Application of RPMI 2650 nasal cell model to a 3D printed apparatus for the testing of drug deposition and permeation of nasal products. *Eur. J. Pharm. Biopharm.* **2016**, 107, 223-233.
53. Bortolotti, F.; Balducci, A.G.; Sonvico, F.; Russo, P.; Colombo, G. In vitro permeation of desmopressin across rabbit nasal mucosa from liquid nasal sprays: the enhancing effect of potassium sorbate. *Eur. J. Pharm. Sci.* **2009**, 37, 36-42.
54. Vaz, G.R.; Hädrich, G.; Bidone, J.; Rodrigues, J.L.; Falkembach, M.C.; Putaux, J.L.; Hort M.A.; Monserrat, J.M.; Varela Junior, A.S.; Teixeira, H.F.; Muccillo-Baisch, A.L.; Horn, A.P.; Dora, C.L. Development of Nasal Lipid Nanocarriers Containing Curcumin for Brain Targeting. *J. Alzheimers Dis.* **2017**, 59, 961-974.
55. Oliveira, P.; Venturini, C.G.; Donida, B.; Poletto, F.S.; Guterres, S.S.; Pohlmann, A.R. An algorithm to determine the mechanism of drug distribution in lipid-core nanocapsule formulations. *Soft Matter*, **2013**, 9, 1141-1150.
56. Bianchin, M.D.; Külkamp-Guerreiro, I.C.; Oliveira, C.P.; Contri, R.V.; Guterres, S.S.; Pohlmann, A.R. Radar charts based on particle sizing as an approach to establish the fingerprints of polymeric nanoparticles in aqueous formulations. *J. Drug Deliv. Sci. Technol.* **2016**, 30, 180-189.
57. Frank, L.A.; Chaves, P.S.; D'Amore, C.M.; Contri, R.V.; Frank, A.G.; Beck, R.C.; Pohlmann, A.R.; Buffon, A.; Guterres, S.S. The use of chitosan as cationic coating or gel vehicle for polymeric nanocapsules: Increasing penetration and adhesion of imiquimod in vaginal tissue. *Eur. J. Pharm. Biopharm*. **2017,** 114, 202-212.
58. Gouda, M.; Elayaan, U.; Youssef, M.M. Synthesis and Biological Activity of Drug Delivery System Based on Chitosan Nanocapsules. *Adv. Nanoparticles*, **2014**, 3, 148-158.
59. Mir, M.; Ishtiaq, S.; Rabia, S.; Khatoon, M.; Zeb, A.; Khan, G.M.; Ur Rehman, A.; Ud Din, F. Nanotechnology: from In Vivo Imaging System to Controlled Drug Delivery. *Nanoscale Res. Lett.* **2017**, 12, 500.
60. Haliza, K.; Alpar, H.O. Development and characterization of chitosan nanoparticles for siRNA delivery. *J. Control. Release* **2006**, 115, 216–225.
61. Sonvico, F.; Cagnani, A.; Rossi, A.; Motta, S.; Di Bari, M.T.; Cavatorta. F.; Alonso, M.J.; Deriu, A.; Colombo, P. Formation of self-organized nanoparticles by lecithin/chitosan ionic interaction. *Int J Pharm*. **2006,** 324, 67-73.
62. Zaki, S.S.O.; Ibrahim, M.N.; Katas, H. Particle Size Affects Concentration-Dependent Cytotoxicity of Chitosan Nanoparticles towards Mouse Hematopoietic Stem Cells. *J. Nanotechnol.* **2015**, 15, 1-5.
63. Huang, M.; Khor, E.; Lim, L.Y. Uptake and cytotoxicity of chitosan molecules and nanoparticles: effects of molecular weight and degree of deacetylation. *Pharm. Res*. **2004**, 21, 344-353.

64. Casettari, L.; Illum, L. Chitosan in nasal delivery systems for therapeutic drugs. *J. Control. Release* **2014**, 190, 189-200.
65. Mazzarino, L.; Coche-Guérente, L.; Labbé, P.; Lemos-Senna, E.; Borsali, R. On the mucoadhesive properties of chitosan-coated polycaprolactone nanoparticles loaded with curcumin using quartz crystal microbalance with dissipation monitoring. *J. Biomed. Nanotechnol*. **2014**, 10, 787-794.
66. Mistry, A.; Stolnik, S.; Illum, L. Nanoparticles for direct nose-to-brain delivery of drugs. *Int. J. Pharm*. **2009**, 379, 146-157.
67. Sosnik, A.J.; Neves, J.; Sarmento, B. Mucoadhesive polymers in the design of nano-drug delivery systems for administration by non-parenteral routes: A review. *Prog. Polym. Sci*. **2014**, 39, 2030-2075.
68. Sigurdsson, H.H.; Kirch, J.; Lehr, C.M. Mucus as a barrier to lipophilic drugs. *Int. J. Pharm.* **2013**, 453, 56-64.
69. Menchicchi, B.; Fuenzalida, J.P.; Bobbili, K.B.; Hensel, A.; Swamy, M.J.; Goycoolea, F.M. Structure of chitosan determines its interactions with mucin. *Biomacromol.* **2014**, 15, 3550-3558.
70. Chaves, P.D.; Ourique, A.F.; Frank, L.A.; Pohlmann, A.R.; Guterres, S.S.; Beck, R.C. Carvedilol-loaded nanocapsules: Mucoadhesive properties and permeability across the sublingual mucosa. *Eur. J. Pharm. Biopharm*. **2017**, 114, 88-95.
71. Singh, I.; Rana, V. Enhancement of Mucoadhesive Property of Polymers for Drug Delivery Applications: A Critical Review. *Rev. Adhesion Adhesives* **2013**, 1, 271-290.
72. Chiou, S.H.; Wu, W.T.; Huang, Y.Y.; Chung, T.W. Effects of the characteristics of chitosan on controlling drug release of chitosan coated PLLA microspheres. *J. Microencapsul*. **2001**, 18, 613-25.
73. Trotta, M.; Cavalli, R.; Chirio, D. Griseofulvin nanosuspension from triacetin-in-water emulsions. *S.T.P. Pharma Sci*. **2003**, 13, 423-426.
74. Zili, Z.; Sfar, S.; Fessi, H. Preparation and characterization of poly-e-caprolactone nanoparticles containing griseofulvin. *Int. J. Pharm*. **2005**, 294, 261-267.
75. Vllasaliu, D.; Exposito-Harris, R.; Heras A.; Casettari, L.; Garnett, M.; Illum, L.; Stolnik S. Tight junction modulation by chitosan nanoparticles: comparison with chitosan solution. *Int. J. Pharm*. **2010**, 15, 183-93.
76. Barbieri,S.; Sonvico, F.; Como, C.; Colombo, G.; Zani, F.; Buttini, F.; Bettini, R.; Rossi, A.; Colombo, P. Lecithin/chitosan controlled release nanopreparations of tamoxifen citrate: loading, enzyme-trigger release and cell uptake. *J Control Release*. **2013**, 167, 276-283.
77. Ahmad, J.; Singhal, M.; Amin, S.; Rizwanullah, M.; Akhter, S.; Kamal, M.A.; Haider, N.; Midoux, P.; Pichon,C. Bile salt stabilized vesicles (Bilosomes): a novel nano-pharmaceutical design for oral delivery of proteins and peptides. *Curr. Pharm. Des*. **2017**, 23, 1575-1588.
78. Colombo, M.; Figueiró, F.; de Fraga Dias, A.; Teixeira, H.F.; Battastini, A.M.O.; Koester, L.S. Kaempferol-loaded mucoadhesive nanoemulsion for intranasal administration reduces glioma growth in vitro. *Int. J. Pharm*. **2018**, 543, 214-223.
79. Khan, A.; Aqil, M.; Imam, S.S.; Ahad, A.; Sultana, Y.; Ali, A.; Khan, K. Temozolomide loaded nano lipid based chitosan hydrogel for nose to brain delivery: Characterization, nasal absorption, histopathology and cell line study. *Int. J. Biol. Macromol*. **2018**, 116, 1260-1267.